Simulating Erosion on Cultural Heritage Monuments

Panagiotis Perakis[1], Christian Schellewald[1], Kidane Fanta Kebremariam[2], and Theoharis Theoharis[1]

[1] Department of Computer and Information Science,
[2] Department of Chemistry,
Norwegian University of Science and Technology (NTNU),
Trondheim, Norway

Abstract. The erosion process is a multi-parametric phenomenon which is hard to simulate algorithmically due to the large number of parameters involved as well as the lack of erosion benchmarking data. Erosion data acquisition is particularly challenging due to the large time-frame involved. Our approach toward building an erosion model for specific types of stone and specific environmental parameters is described as well as the acquisition of erosion data from specialized accelerated erosion chambers. The stone types addressed are marble and soapstone. We obtain data from the erosion chambers which simulate atmospheric pollutants, the effect of salt intrusion as well as the freeze-thaw effect. Once a cultural heritage monument is scanned in 3D, the erosion simulator can be used to perform sensitivity analysis on the effect of erosion based on the variation of the input parameter values. This analysis can show the degree of danger that the cultural heritage monument is in, according to the assumed parametric values. Erosion values are mapped onto the 3D scan of the cultural heritage monument and their visual nature is useful for the public dissemination of the involved danger. According to our records, this is the only detailed erosion simulator for stone. This work is supported by the European Unions Seventh Framework Programme (FP7/2007-2013) under grant agreement no 600533 PRESIOUS (www.presious.eu).

Keywords: Cultural Heritage, Accelerated Erosion Chambers, Erosion Benchmarking, Erosion Simulation.

The Demeter Sanctuary in Elefsis, Greece

The Nidaros Cathedral in Trondheim, Norway

Fig. 1. The two Cultural Heritage Monuments under study.

1 Introduction

The computer simulation of the naturally occurring stone degradation process is very attractive because it could enable us to predict the future state of important Cultural Heritage (CH) monuments based on different

environment scenarios and thus allow us to take appropriate action in good time. The purpose of this study is to contribute to the simulation of the fundamental and most common degradation mechanisms that impact objects that are built out of stone. Our ultimate aim is to model and simulate the physico-chemical processes that lead to the degradation of the stone-material of CH objects over time. Towards this aim we are implementing a prototype software application that simulates surface mesh alterations of CH objects and allows therefore to imitate manifestations of stone degradation phenomena like surface recession and crust formation.

The three main degradation processes which often work simultaneously to decompose rocks are *physical/mechanical*, *chemical* and *biological* in nature. One of the main causes of stone decay is the interaction between water and the porous structure. Water absorption can induce weathering on stone materials in several ways:

1. by **chemical reaction** with industrial pollutants, mainly the atmospheric gases of carbon dioxide CO_2, sulfur dioxide SO_2 and nitrogen dioxide NO_2, which decay the stone material by changing its chemical composition;
2. by a physical mechanism through **mechanical stresses** due to freeze/thaw and wet/dry cycles, that disintegrate stones into smaller particles, which are then removed by gravity, wind, water or ice;
3. by acting as a transport medium for **salts** in dissolution and recrystallization processes within the pore space;
4. by providing an essential substrate for **biological growth** of living organisms such as bacteria, fungi, algae and lichens.

Stone decay appears in many different forms. Stone may gradually and slowly weather away, leaving a solid surface behind. At other times sheets or flakes break off from the stone at once. Sometimes the surface starts to show blisters or a stone just loses its integrity and crumbles away. Some of the stones can appear perfectly intact for a long time while already losing cohesion underneath.

The small amount of recession rates observed at cultural heritage sites, the complexity of the deterioration mechanisms, the unavailability of chemical data that characterize the monument building materials on site, and the uncontrolled environmental conditions, make it necessary to setup accelerated erosion chambers for conducting specific purpose experiments, under controlled conditions using chemically characterized stone samples. These experiments will provide the necessary bench-marking of the parameter values that that drive the erosion process and its modelling.

2 Related Work

Although there is much work that has be done concerning in situ studies of the physicochemical processes of stone erosion and their significance to the conservation treatments of Cultural Heritage objects, the construction of accelerated erosion chambers and the conduction of specific purpose experiments, under controlled laboratory conditions is a rather under-studied issue - see the excellent survey of E. Doehne and C. Price concerning the current research on stone decay and conservation (Doehne & Price 2010), and the state-of-the-art report of C. Schellewald *et al.* concerning the simulation of stone deterioration processes (Schellewald, Theoharis, Gebremariam & Kvittingen 2013).

Gauri, Yerrapragada, Bandyopadhyay *et al.* in a series of works (Yerrapragada, Jaynes, Chirra & Gauri 1994), (Yerrapragada, Chirra, Jaynes, Li, Bandyopadhyay & Gauri 1996) and (Gauri & Bandyopadhyay 1999) described the erosion on carbonate stones, and especially marble, under polluted and unpolluted, dry or wet environments. Given that the mechanisms of surface recession and crust creation are too complex, the authors set up chemical erosion chambers to study the effects of CO_2, SO_2 and NO_2 in dry or wet controlled conditions. They also made outdoor experiments measuring the amount of material that runs off during rain showers and related this to the exposed sample surface allowing them to estimate the recession under rainfall. The chemical processes were modeled by the unreacted-core model, which led to the calculation of the crust deposition rate in dry environments or the surface recession rate by acid rain.

G. W. Scherer examined several important weathering processes like the thermal expansion of calcite, freeze/thaw cycles, salt crystallization along with the swelling of clay inclusions (Scherer 2006). He reviewed these weathering mechanisms and outlined which aspects remain to be solved. He concluded that salt damage is one of the most serious, but least understood, causes of stone deterioration and that the essential mechanisms that cause stresses in stone are known, but that details are not clear.

D. G. Price noted that chemical weathering usually includes the solution of stone material, the degree of which depends on the amount of water passing over the surface, the solubility of the material, and the pH

value of the water (Price 1995). Considering all possible reactions of stone materials with all possibly present chemicals becomes quickly very complex. However, for some stones the chemical degradation or weathering mechanisms of particular material components are relatively well known.

The effects of ozone and NO_x on the deterioration of calcareous stone was investigated by S. W. Massey. He investigated the effects of these gases on the deterioration of different stones in chamber reactions and field works in urban and rural environments (Massey 1999).

The corrosive effects of gaseous SO_2, NO_x, O_3, HNO_3, particulate matter, and acid rainfall are the topic of C. Varotsos *et al.* , concerned with the enhanced deterioration of the cultural heritage monuments (Varotsos, Tzanis & Cracknell 2009).

A. Moropoulou *et al.* presented in (Moropoulou, Bisbikou, Torfs, van Grieken, Zezza & Macri 1998) weathering phenomena on Pentelic marbles at the Demeter Sanctuary in Elefsis, Greece. A systematic mineralogical, petrographical and chemical examination of weathered stones and crusts was performed, both in situ and in the lab, on samples taken from different parts of the monument in relation to the surface characteristics as well as to the exposure to rain, sea-salt spray and wet and dry deposition of airborne pollutants and dust.

P. Storemyr in a series of works (Storemyr 1997), (Storemyr, Wendler & Zehnder 2001) and (Storemyr 2004) presented weathering phenomena at the Nidaros cathedral in Trondheim, Norway. He noted that stones from eight quarries are used in the monument and he presented and compared the behavior in weathering and conservation of the respective stone types (soapstone and greenschist). Storemyr discussed the geology, petrography and salt content of soapstone deposits. According to Storemyr the "Grytdal" stone seems also to contribute to the formation of black gypsum crusts as the observed crusts can not be attributed to air pollutants (SO_2 and particulate matter) alone.

3 Erosion Measurements

3.1 Erosion Measurements at the Cultural Heritage Sites

For the investigation of the erosion mechanisms that contribute to the degradation of stones, we collected 3D geometric data from the two Cultural Heritage sites, the Demeter Sanctuary in Elefsis, Greece, and the Nidaros Cathedral in Trondheim, Norway (Figure 1). Figure 2 (b) shows the result mesh of the geometric scan of the Elefsis-pillar that took place at Elefsis in March 2013. The areas of the Elefsis-pillar, that are marked with boxes, indicate the patches we selected for illustration of measurements and investigations. The geometric scans were repeated in 2014 and 2015.

At the Nidaros Cathedral several smaller areas were selected for scanning. These include two wall parts from the Lectorium (Lectorium East, with Mason Marks, and Lectorium North) and two scans from the inside of the North West and South West Tower of the Cathedral. In Figure 2 (a) we illustrate the geometric scan of the east wall of the Lectorium that contains two mason marks. A close-up view of the area with a mason mark is depicted as well.

The "Differential Geometry Measurer" is the module within our erosion simulation software that aligns and measures the erosion of stone surface areas that are scanned consecutively at the cultural heritage sites (Figure 3) or alternatively using the stone slabs exposed to accelerated erosion (Figure 11).

3.2 Accelerated Erosion Experiments

The unavailability of chemical data and the small amount of recession observed at the Cultural Heritage sites themselves (Figure 3), made it necessary to complement these measurements with data obtained from accelerated erosion experiments, that study erosion parameters in isolation. Considered weathering experiments include effects that originate from polluted environments and from naturally occurring climatic conditions. The experiments that we finally decided to perform, include the Salt effect (using sodium sulfate Na_2SO_4), the Freeze-and-Thaw effect, that simulate mechanical effects and two chemical experiments simulating polluted industrial environments, rich in SO_2 and NO_2 (using aqueous solutions of sulfuric acid H_2SO_4(aq) and combined sulfuric and nitric acid H_2SO_4+HNO_3(aq)).

In addition to the Salt and Freeze-and-Thaw weathering experiments, the acid weathering experiments were carried out to study the effects of polluting gases such as SO_2 and NO_2 in solution form. Cyclic soaking experiments in acidic solutions of sulphuric and nitric acids, with alternating wetting and drying stages, were used to simulate the accelerated weathering. Physicochemical changes at macroscopic and microscopic levels were monitored through characterizations using multiple analytical techniques.

In the following sections we describe the created accelerated erosion chambers and the performed experiments.

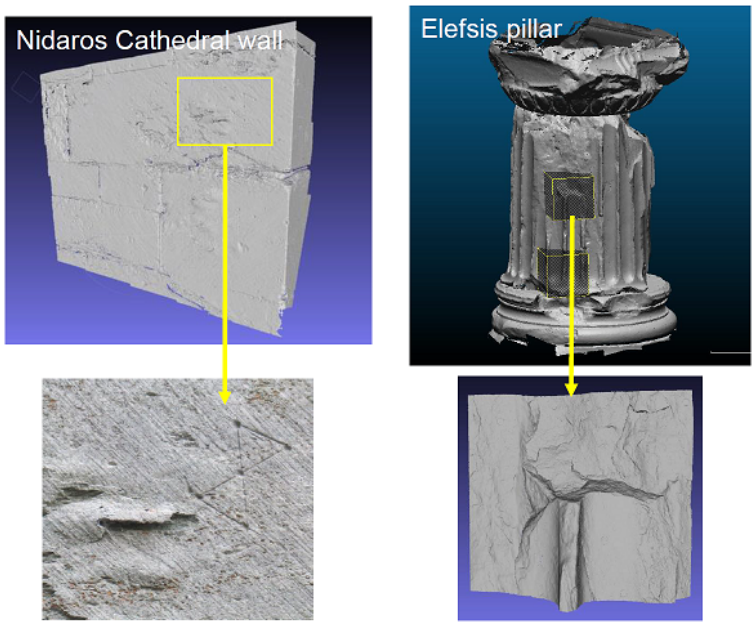

Fig. 2. Scanned geometric meshes from the two Monuments. (a) The scanned Nidaros-wall and a patch showing in more detail the X mason mark that is present on the east wall of the Lectorium of the Nidaros Cathedral; (b) The scanned Elefsis-pillar and a patch showing in more detail the column area inside the upper box.

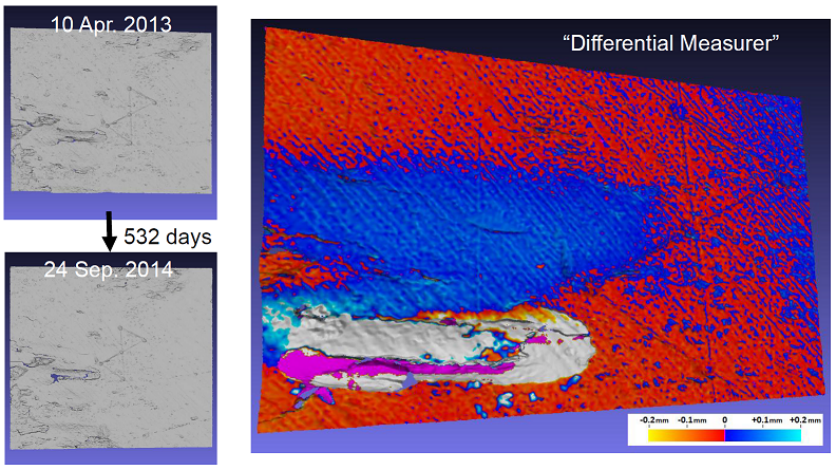

Fig. 3. The "Differential Measurer" computes the distance map between two scanned meshes; here the 3D geometry meshes of the two X mason mark patches of Round 01 (2013-04-10) and Round 02 (2014-09-24) scans are depicted. The meshes are at first registered, and then distances are computed and mapped as textures onto the Round 01 mesh.

Stone Slabs and their Labeling The stone samples that were used in the experiments carried out in our accelerated erosion chambers are stone slabs similar to the stones used at the two Cultural Heritage sites; the Demeter Sanctuary in Elefsis, Greece, and the Nidaros Cathedral in Trondheim, Norway (Figure 1). Pentelic marble was used at the Demeter Sanctuary (Moropoulou et al. 1998) and Grytdal soapstone was used in the Nidaros Cathedral (Storemyr 1997). The stone slabs were named according to their origin (Elefsis, Nidaros); furthermore the soapstone slabs labelled with reference to the stone quality (Good, Bad) and finally according to their size (Large, Small) (see Figure 4). Details concerning the labeling of the specific stone samples used in each of the erosion experiments are listed in Table 6.

Pentelic Marble: dense metamorphic rock; homogeneous; almost entirely made of calcite (96% $CaCO_3$); with low porosity (3.64 $vol\%$) (Moropoulou et al. 1998).

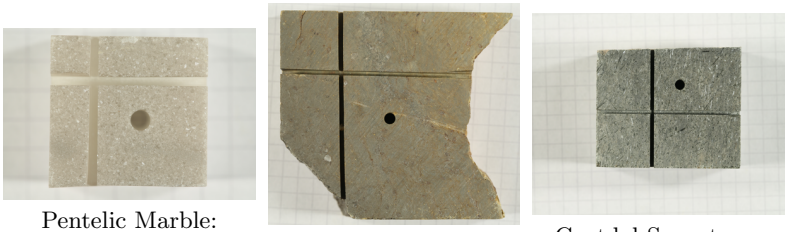

Pentelic Marble: Elefsis Large 01

Grytdal Soapstone: Nidaros Bad Large 01

Grytdal Soapstone: Nidaros Good Large 01

Fig. 4. Photos of some stone slabs used in the accelerated erosion experiments.

Grytdal Soapstone: dense metamorphic rock; non homogeneous; made mostly of chlorite $(20\% - 60\%)$ and talc $(5\% - 20\%)$; with low porosity $(3.60\ vol\%)$ (Storemyr 1997).

Acid Chambers For simulating acid rain in an accelerated weathering experiment two acidic conditions were selected: Sulfuric acid weathering (H_2SO_4) and combined Sulfuric/Nitric acid weathering (H_2SO_4+HNO_3); the first one to simulate the effects of acid rain due to SO_2 concentrations and the second one due to combined SO_2 and NO_2 concentrations. In one cycle the stones are subsequently submerged for a prolonged time ($\approx 5\ days$) in chemical solutions and dried right afterwards ($\approx 24\ hours$). The purpose of these periodic shocking experiments, with alternating wetting and drying steps, is to simulate accelerated acid weathering conditions.

(a) H_2SO_4(aq)

(b) H_2SO_4+HNO_3(aq)

Fig. 5. Experimental setup for acid weathering. The solutions are mixtures of H_2SO_4 and HNO_3.

Sulfuric Acid Chambers (H_2SO_4(aq)) For this experiment an acid solution, H_2SO_4, of pH 4 was prepared from reagent grade concentrated sulphuric acid. In each weathering container three samples from the same type of stone were totally immersed in the solution. The volumes of the solution for each group of identical stone types, Elefsis, Nidaros Good and Nidaros Bad, were 4 L each, kept in plastic containers of 7 L in size (Figure 5 (a)). The containers were closed during the soaking phase to minimize the effect of evaporation.

The pH of the solution was adjusted on daily basis using a 0.1 M solution of H_2SO_4. The pH measurements were made through the use of a pH meter (Jenway, model 3510 pH meter). The weathering experiment was conducted at room temperature and humidity. The CO_2 level in the laboratory was continuously measured with a help of a CO_2 data logger. ZyAura ZG1683RU CO_2 monitor was used for this purpose along with ZG Series application software for real-time data analysis, calibration, etc.

After 5 days intervals on average, the samples were taken out of the solution, and dried for 24 hours at $105°C$ in a desiccator and weighted afterwards. The stones were exposed to the simulated acidic solutions for a period of one month and 10 days in the first round before characterization.

Combined Sulfuric/Nitric Acid Chambers (H_2SO_4+HNO_3(aq)) The acid solution was prepared by mixing H_2SO_4 and HNO_3 solutions in the ratio of 2/3 and adjusting the pH to 4. The solutions are intended to simulate acid rain. The chemicals used are all reagent grade. The volumes of the solution for each group of identical stone types, Elefsis, Nidaros Good and Nidaros Bad, were 4 L each kept in a closed plastic container of 7 L in size (Figure 5 (b)). The stones were immersed in the solution with the pH adjusted at 4 on a daily basis using a 0.1 M solution of HNO_3.

The weathering experiment was conducted at room temperature and humidity. The CO_2 level in the laboratory was continuously measured with a help of a CO_2 data logger.

The samples were taken out of the solution, dried for 24 *hours* and weighted after every 5 *days* on average. In the first round, the weathering processes continued for a period of one month before characterization of the stones by multi-analytical techniques.

Salt and Freeze-and-Thaw Chambers In order to investigate the Salt, and the Freeze-and-Thaw effects, we designed and constructed two erosion chambers for our accelerated erosion experiments. They are controlled by Arduino micro-controllers (Arduino LLC 2015) and continuous measurements are taken over USB connections. Typical curves that originate from 24 *hour* measurements from both chambers are shown in Figure 8.

Salt Chamber One cycle within the Salt Chamber takes 6 hours and consists of submerging the stones in the salt solution, of Na_2SO_4 decahydrate, for 3 hours and drying them for 3 hours in a constant light airflow created by small fans attached to the chamber. Note that 3 hours is the amount of time taken for the chambers to enter into a steady state of humidity variation. Figure 6 shows the Salt Chamber in both states. The left image shows the stones lifted up. The white crust indicates that the stones already dried for a while. On the right image, the stones are submerged within the salt solution. The temperature and humidity of the chamber is continuously monitored over the lifetime of the experiments (Figure 8 (a)).

The first round of accelerated Salt effect erosion started on 19th September 2014 and was stopped on 21st October 2014, and lasted for 32 *days* having 128 *cycles* of $21,600$ *sec* (wetting: $10,800$ s - drying: $10,800$ s).

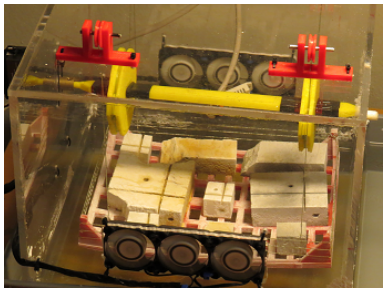

Salt Chamber
with stones being dried
(Dry phase)

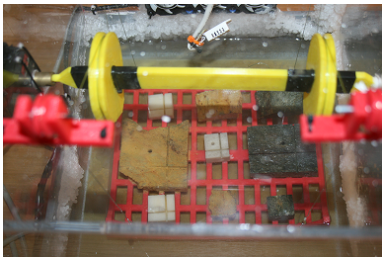

Salt Chamber
with stones submerged
(Wet phase)

Fig. 6. The Salt Chamber shown at two different cycles and states. Dry and wet phases change every three hours during the accelerated erosion cycles.

Freeze-and-Thaw Chamber The Freeze-and-Thaw Chamber is constructed out of a small refrigerator and a water purification system that are both controlled by an Arduino micro-controller. Figure 7 shows the Freeze-and-Thaw Chamber uncovered and covered with the rain basin which is supplied with purified water to simulate rain drops falling. One cycle within the Freeze-and-Thaw Chamber takes 8 hours. This includes 3 *hours* of freezing and 5 *hours* of warming up. The length of the warm cycle was selected so that the chamber reaches a temperature of about $5°C$. The freezing cycle guarantees a long state where the temperature is below $-5°C$. Within the last 30 *minutes* of the warming phase, purified water drops onto the stones. For this chamber we used a separate Arduino for continuously measuring the temperature (Figure 8 (b)).

The first round of the accelerated Freeze-and-Thaw erosion started on the 10th of November 2014 and ended on the 4th of December 2014, and lasted for 24 *days*, having 72 *cycles* of $28,800$ *sec* (warming: $18,000$ *s*, incl. $1,800$ *s* rain - freezing: $10,800$ *s*).

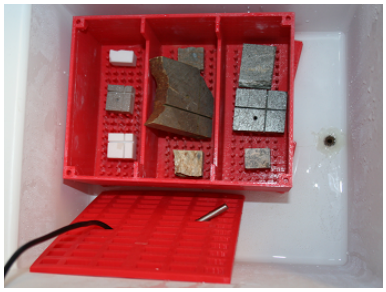

Freeze-and-Thaw Chamber
stone compartments
(uncovered)

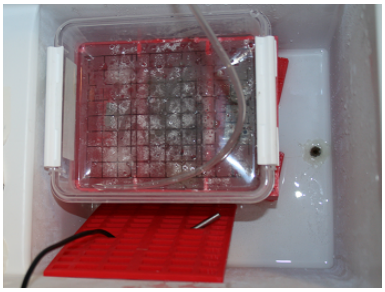

Freeze-and-Thaw Chamber
stone compartments
(covered with rain basin)

Fig. 7. The inner structure of the Freeze-Thaw Chamber. Before a freezing cycle starts, purified water drops for 30 minutes onto the stones, simulating rain.

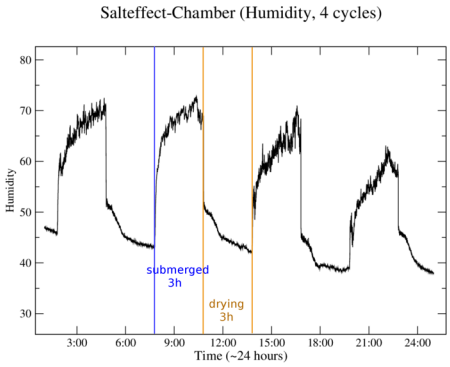

Salt Chamber:
Humidity data
(2014-10-14)

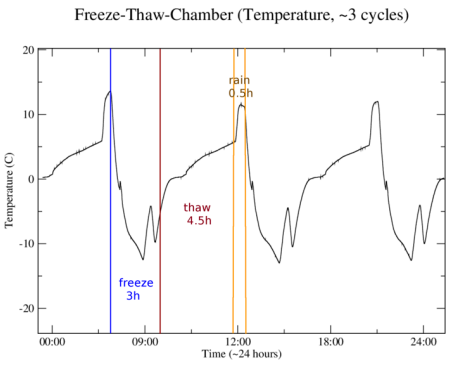

Freeze-and-Thaw Chamber:
Temperature data
(2014-11-20)

Fig. 8. Typical measurements gathered during the accelerated erosion experiments in the Salt and Freeze-and-Thaw Chambers.

3.3 Measurement modalities

Several measurement techniques are used to characterize the changes that occur on the stone samples during the accelerated erosion cycles. The measurements consist of mass measurements, 3D Geometric Scans, Quantitative Evaluation of Minerals by SCANning electron microscopy (QEMSCAN), Scanning Electron Microscopy with

X-ray microanalysis (SEM-EDS), 3D microscopy, micro Computed Tomography (micro-CT), X-Ray Diffraction (XRD) and Petrography. The data sets currently collected from these measurements which are also used as input data of the Erosion Simulator are summarized below.

3D Geometry Scans The 3D scans of the stone slabs in high resolution surface meshes of the 3D geometry of the stones, were performed by Aicon – our industrial partner in the PRESIOUS project – using a Breuckmann Scanner (AICON 3D systems 2015). An example of the resulting mesh data is depicted in Figure 9.

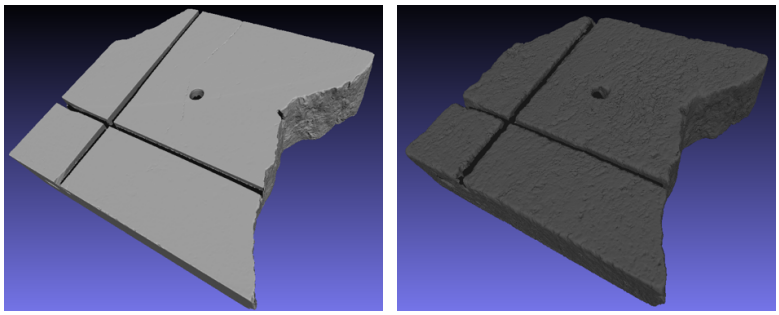

Round 01 (2014-06-02) Round 02 (2015-01-12)

Fig. 9. Depiction of the 3D scans of the Nidaros Bad Large 02 stone slab; Notice the roughness of the surface of the Round 02 scan compared to that of Round 01 due to the erosion.

QEMSCAN Quantitative Evaluation of Minerals by SCANning electron microscopy is a technique that uses a Scanning Electron Microscope (SEM) combined with X-ray spectroscopy and a database to obtain accurate mineral maps for a measured stone surface, performed by Robertson CGG (Robertson CGG 2015). The results of the QEMSCAN of some of the stone slabs is shown in Figure 10. The used color codes and labeling of the mineral map is also depicted.

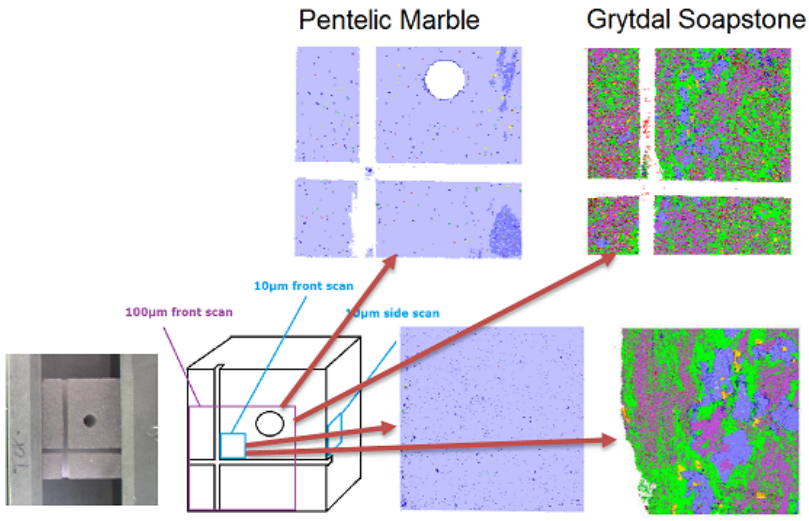

Color Coded Mineral Map

Minerals	Color	RGB-dec		
Quartz		255	255	0
K-Feldspar		221	160	221
Plagioclase Feldspar		255	105	180
Biotite		128	0	0
Illite		0	192	0
Chlorite		0	255	0
Smectite		51	102	0
Kaolinite		192	64	0
Glauconite		128	128	0
Calcite		192	192	255
Dolomite		128	128	255
Ankerite		255	192	128
Siderite		255	128	0
Gypsum/Anhydrite		178	34	34
Pyrite		255	215	0
Heavy Minerals		255	0	0
Altered Mafics		186	85	211
Pores		0	0	192
Others		128	128	128
No measurement		255	255	255

Fig. 10. Depiction of the mineral maps from the QEMSCAN of "Pentelic Marble" and "Grytdal Soapstone" stone slabs; Table of color codes of minerals that appear in the QEMSCAN mineral maps.

3.4 Estimation of the extent of erosion between Erosion Cycles

Mass measurements After removal of the samples from the Salt Chamber, the stone samples were rinsed thoroughly with deionized water, dried for 24 *hours* at 105°C and cooled to room temperature in a desiccator before mass measurements. The same procedure, except rinsing with deionized water, was followed for the stone samples from the Freeze-and-Thaw Chamber. For the Acid Chambers, the samples were taken out of the solution, dried for 24 *hours* at 105°C and cooled to room temperature in a desiccator before weighting.

Mass measurements confirm our observation that stones from Nidaros (i.e. NBL1 and NBL2) suffer more erosion than the other stones and also that the Salt effects are more dramatic than the Freeze-Thaw effects, even worse than the Acidic effects (see Table 6).

Estimating mean erosion using micro-CT scans and surface scans One way of estimating the mean erosion rate δ is to use the surface areas S_1 and S_2 of the mesh and the corresponding volumes V_1 and V_2 of the stone slabs before (Round 01) and after erosion (Round 02) respectively. Assuming that the surface area doesn't change too much we can use the differential equation $\Delta V = S\Delta h$, and $\delta = \Delta h = \Delta V/S$, where $\Delta V = V_2 - V_1$ and $S = S_{avg} = (S_1 + S_2)/2$.

The surface areas S were computed using the summation of the triangles area of the scanned mesh. The volumes V_1 and V_2 were computed counting the non-void voxels of the micro-CT scans of the slabs. Since the micro-CT data did in some cases not cover the whole volume of the slabs (in particular the larger stone slabs did not fit into the measurement space) during the first round (Round 01) measurements, V_1 could not be directly computed from them, so finally it was computed from the first round mass m_1 using the second round density ρ_2, which was considered constant between the two cycles.

We have estimated the mean erosion δ using the previously described method and the results for the various slabs are presented in Table 6. Note that stone slabs NBL3 and NBS1 under acid weathering exhibit swelling which overcomes the recession of material from their surfaces. Stone slabs NGL3 and NGS1 under acid weathering exhibit swelling as well but not so intense which almost equalizes the recession of material from their surfaces. This swelling phenomenon exhibited on Grytdal soapstones has to be further investigated.

Estimating erosion on every vertex of the stone mesh A key problem in measuring erosion based on scans made across time is the difficulty in registering these scans. Due to the absence of an external reference frame, a typical registration algorithm, such as Iterative Closest Point (ICP) (Besl & McKay 1992), will align the scans so as to minimise the RMS error between them, which is not an ideal solution in case of erosion, since it diminishes the common erosion that has to be measured. Thus for the case of the large monumental scans for which we do not have any other information except the surface mesh, the two consecutive scans are at first registered using ICP and then the per vertex erosion is computed in a relative manner having positive and negative values with respect to the reference mesh (see Figure 3). The same is actually true for the stone slabs (see Figure 11 (a)).

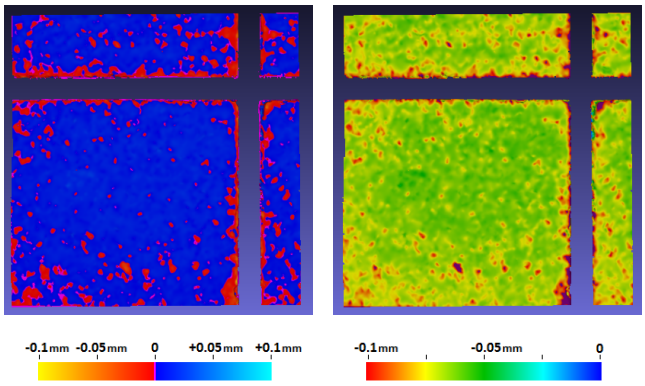

(a) (b)

Fig. 11. Differential Map of initial to eroded mesh for the frontal surface of the stone slab Elefsis Large 3 (EL3): (a) Slabs registered using ICP (blue indicates positive distances and red indicates negative distances); and (b) Slabs displaced in Z using estimated erosion value (red indicates most eroded areas and blue least eroded areas).

Here is how we handled this problem in the case of the stone slabs used in the accelerated erosion experiments. We first register the top surface of the slabs using ICP and assume that this registration is sufficient in terms of the X and Y dimensions that define the top surface. Then we translated the surface mesh by a displacement in Z direction that equals the computed mean erosion δ that is estimated by the previously described method (see Figure 11 (b)).

Consider two point sets $M = \{\mathbf{m}_1, \mathbf{m}_2, \ldots, \mathbf{m}_p\}$, that represents the initial surface of a stone, and $T = \{\mathbf{t}_1, \mathbf{t}_2, \ldots, \mathbf{t}_q\}$ that represents the weathered surface of the same stone, where $\mathbf{m}_i,\ \mathbf{t}_j \in \mathbb{R}^3$. The distance $d_e(\mathbf{m}_i) = \min_j(\|\mathbf{m}_i - \mathbf{t}_j\|)$ can be used as a local erosion measure which expresses at each vertex of the initial model M the distance of the closest vertex of the eroded model T, and is a scalar mapping of the erosion measure at each vertex of the initial stone model M, to which the eroded model T is registered. $\|\mathbf{m}_i - \mathbf{t}_j\|$ is the Euclidean distance of a point of M from a point of T.

Figure 11 depicts the distance maps (i.e. the $d_e(\mathbf{m}_i)$) between the Round 01 and Round 02 meshes of Elefsis Large 3, and consequently the computed by he "Differential Geometry Measurer" erosion measure textured on the initial mesh as a distance map. In Figure 11 (a) the distance map after the ICP registration is depicted, and in Figure 11 (b) the distance map after the Z-shift correction that equals mean erosion δ. In Figure 3 the distance map between the Round 01 and Round 02 of the X mason mark scanned patch, which is present on the east wall of the Lectorium of the Nidaros Cathedral, is depicted; the meshes are at first registered, and then distances are computed and mapped as textures onto the Round 01 mesh.

4 The Erosion Simulator

4.1 Description of the Erosion Simulator

The purpose of the Erosion Simulator is the simulation of the fundamental and most important degradation mechanisms that impact objects that are made of stone. Therefore the simulator aims to model and simulate the physico-chemical processes that lead to the degradation of the stone-material over time. Towards this aim we implemented a prototype for the mesh alteration that acts on the surface geometry and allows therefore to imitate the surface recession or crust growing. The erosion engine implements a mesh off-setting model. This model relies on a computational and a physico-chemical model, which will be subsequently described.

4.2 Modeling Stone Weathering

The main weathering processes responsible for the erosion of rocks and stones are of chemical and physical nature. **Chemical weathering** *describes the decay of the stone material into new chemical products by the chemical reactions of the stone material with water and atmospheric gases like carbon dioxide (CO_2), sulfur dioxide (SO_2) and nitrogen dioxide (NO_2).* The two different chemical weathering scenarios that are usually distinguished are the weathering within a natural environment and the weathering within a polluted environment. The first (unpolluted) scenario considers (beside the air) only the gas carbon dioxide (CO_2) while the second scenario contains also the industrial gases sulfur and nitrogen dioxide (SO_2 and NO_2). The chemical weathering results in two main effects; the gain or loss of material. The first one is mostly visible as crust building up on surfaces while the second one relates in most cases to surface recession. The crust formation is usually due to the deposition of chemical material in polluted environments while the loss of material results mainly due to reactions of water with the stone-material and pollution gases. The chemical products in this process are subsequently washed away. Temperature and humidity play crucial roles in these processes (Gauri & Bandyopadhyay 1999).

Physical or **mechanical weathering** *describes the disintegration of the stone material into smaller particles under the action of heat, water and pressure on the stone, which then can be removed by gravity, wind, water or ice.* The two different mechanical weathering scenarios that are usually distinguished are the weathering caused by soluble salts and the weathering caused by wet/dry and freeze/thaw cycles. Along with air pollution, soluble salts represent one of the most important causes of stone decay. Salts cause damage to stone in several ways. The most important is the growth of salt crystals within the pores, fissures and cracks of a stone, which can generate stresses that are sufficient to overcome the stone's tensile strength and turn the stone to fragmented pieces. Another important decay mechanism under the general term "differential stress" includes the effects of wet/dry cycling, clay swelling, differential hygric stress, differential thermal stress, and stress from differential expansion rates of material in pores (such as salts or organic material) versus in the stone (Doehne & Price 2010).

4.3 Modeling Mesh Alteration

The formulas which describe the surface weathering provide usually a measure for the change of the surface geometry (deposition/recession δ) of the object surface which depends on the environmental parameters (such as the amount of rain fall, the concentrations of the involved pollution gases, the temperature, the humidity etc.) and the stone material. This suggests a simple procedure to simulate erosion acting just on the object surface mesh: For each vertex of the surface mesh one has to calculate the recession rate of the erosion according to the various environmental parameters with adoptions to the local stone material parameters. Then the surface mesh change is performed along the normal direction of the surface.

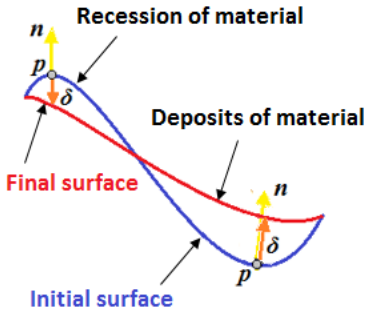

Fig. 12. Modeling of an erosion process on the surface of a stone.

Geometric Model of Erosion Defining the initial surface of a stone as a set of 3D points $S = \{\mathbf{p}_1, \mathbf{p}_2, \ldots, \mathbf{p}_n\}$ and the weathered surface of the same stone in a similar way as $S' = \{\mathbf{p}'_1, \mathbf{p}'_2, \ldots, \mathbf{p}'_n\}$ with $\mathbf{p}_i,\ \mathbf{p}'_j \in \mathbb{R}^3$ one can describe the surface deposition/recession as an offsetting procedure with the help of the diffusion equation.

The diffusion equation

$$\frac{\partial \mathbf{p}}{\partial t} = \mu \nabla^2 \mathbf{p} = \delta \mathbf{n} \ , \tag{1}$$

leads to a simple update rule for computing the offset of the mesh vertices $\mathbf{p}_i$

1. iterate
2. $\mathbf{p}'_i = \mathbf{p}_i + \delta_i \ \mathbf{n}_i \ dt$,
3. until # of epochs (of dt duration each)

Here $\mathbf{n}_i$ is the normal vector at the surface vertex $\mathbf{p}_i$ and δ_i is the surface recession ($\delta_i < 0$) or deposition ($\delta_i > 0$) at this point (see Figure 12). The corresponding time interval of each epoch is denoted as dt. *Epochs* denote time intervals were different environmental conditions, such as pollution concentration and/or rain fall, can be defined. The number of epochs denotes the total time over which the object is exposed to weathering.

Physico-Chemical Model of Erosion The value of the surface off-setting rate δ_i is going to be determined by the accelerated erosion experiments. The theoretical background of the chemical processes are modeled by the unreacted-core model, which leads to the computation of the mesh offsetting δ for the cases of dry deposition of crust due to $SO_2 + NO_2$ and surface recession by acid rain due to $SO_2 + NO_2 + CO_2$ is described in detail in (Gauri & Bandyopadhyay 1999, Yerrapragada et al. 1996, Yerrapragada et al. 1994). Note how dramatically high the recession rates due to acid rain are, compared to the deposition rates of crust in dry environments. This result reaffirms that acid rain recession is the most significant component in the erosion model.

4.4 Erosion Simulator Processing Modes

According to the data types that are available to the "Erosion Simulator" module, it can run in two different processing modes.

Application of the Erosion Simulator on a mesh of homogeneous stone In this first mode, the input of the Erosion Simulator is 3D geometric surface data only, in a mesh structure. The Erosion Simulator considers that data come from a homogeneous stone of a known type. The Erosion Simulator produces the eroded surface geometry considering that δ for deposition/recession *is the same on every vertex of the mesh*, determined by the stone type and the environmental parameters.

The 3D geometric surface data are available for large areas - such as from the Elefsis pillar or the Nidaros Cathedral walls - where no other extra information for the mineral composition of the surface is available. But it can also be applied to the 3D geometric surface data of the stone slabs by just ignoring the extra mineral composition information of the QEMSCANs. In this mode, the simulator runs on various complete irregular or regular meshes acquired at different resolutions. Our scanned datasets have mean-edge-length at $0.060 \sim 0.098\ mm$.

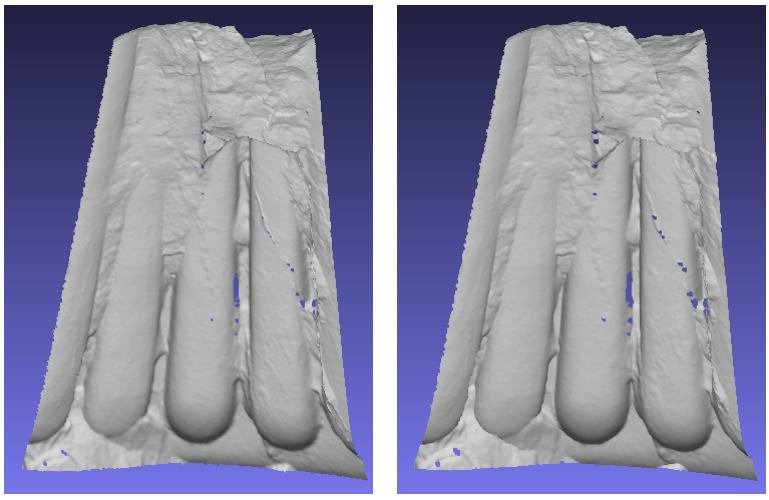

(a) **(b)**

Fig. 13. Modeling of an erosion process on the surface of Elefsis pillar: (a) original stone surface; and (b) weathered (thinned) stone surface due to acid rain recession over a period of 200 years.

For example the implementation of this fundamental surface offsetting model is applied to the surface mesh of the Elefsis pillar. The effect of this thinning process is depicted in Figure 13. The result simulates the acid rain recession on marble, under certain environmental conditions over a period of 200 years, yielding a surface offset of almost 3.4 mm. The computation of the recession rate is an implementation of the (Gauri & Bandyopadhyay 1999) model.

Application of the Erosion Simulator on a mesh textured with a mineral map The physico-chemical aspects of the erosion involves geometrical information and physicochemical data on the surface of the object being eroded. In this second mode, the input of the Erosion Simulator involves geometric information in the form of a mesh and mineral data assigned on the surface of the object being eroded. The surface physico-chemical data of the stone slabs can be created by registering the available 3D scanned meshes and the QEMSCAN texture information. The Erosion Simulator produces the eroded surface geometry considering that δ for deposition/recession *is different on every vertex of the mesh*, and is determined by the mineral type assigned to it and the environmental parameters. δ dependencies on mineral attributes have to be determined by experimental data.

A crucial first step for this procedure is the registration of the acquired geometric mesh data with the QEMSCAN mineral map texture data (Figure 14). The general registration transformation matches landmark points annotated on the geometry image of the scanned 3D mesh, and the corresponding landmark points annotated on the QEMSCAN texture, which are considered as the invariant reference points under the correspondence transformation. These points are localized using the hole and the cross which are engraved onto the slabs for this purpose.

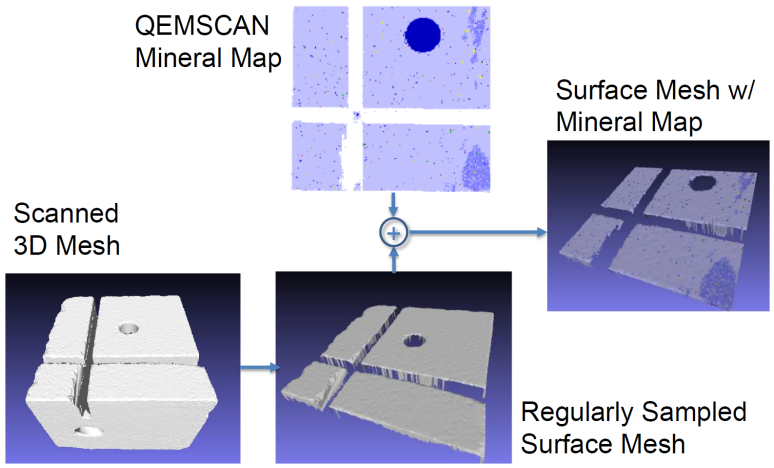

Fig. 14. Depiction of 3D geometry and QEMSCAN registration results for the Elefsis Large 1 (EL1) marble slab.

In this mode, the simulator runs on various regular meshes re-sampled at different resolutions and textured with the QEMSCAN mineral map images. Our datasets after regular resampling have mean-edge-length at $0.035 \sim 0.050\ mm$

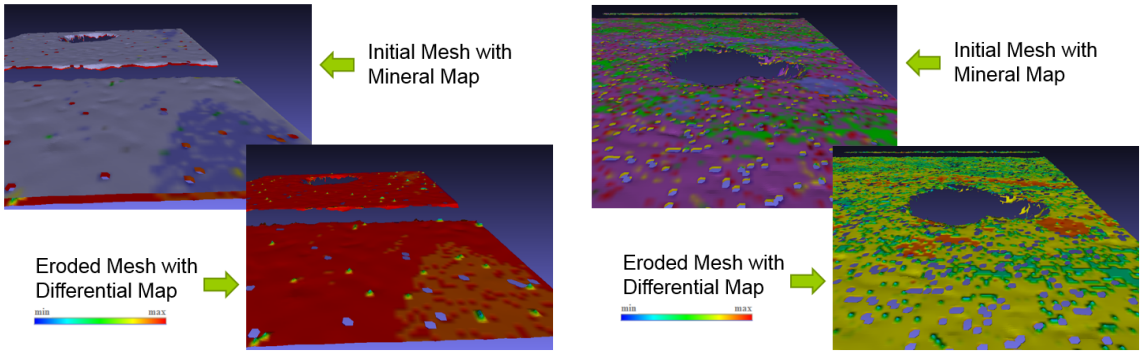

(a) Elefsis Large 1 (EL1)

(b) Nidaros Good Large 2 (NGL2)

Fig. 15. Erosion prediction for two stone slab surfaces (red indicates most eroded areas and blue least eroded areas).

Although the Erosion Simulator is currently in a version which can deal with the combination of geometric mesh data along with registered mineral map texture, the physico-chemical model that drives this per-mineral erosion computation is not completed yet. This will be done by enhancing the Gauri model for calcium carbonate stones (Gauri & Bandyopadhyay 1999) also for other minerals, by statistically determining the erosion rate δ, analysing the results of the accelerated erosion experiments and the on-site erosion measurements.

The predictions of the Erosion Simulator are depicted in Figure 15, by just applying a different offset values at vertices having different mineral composition according to the conjecture that some minerals will be eroded more and some less.

5 Concluding remarks

This paper describes the design and implementation of a prototype software application that simulates surface mesh alterations of Cultural Heritage objects and allows therefore to imitate manifestations of stone degradation phenomena like surface recession and crust formation. However, a simulation of this type proved to be extremely challenging, both because of the large number of parameters involved and because of the difficulty involved in bench-marking these parameters with actual experimental data values. Simulating all the natural effects that

contribute to erosion is rather chaotic and also a long term process, thus we tried to focus on the most important effects and tried to simulate these experimentally in isolation for the specific stone types that were used in the two Cultural Heritage sites we are studying, i.e. Pentelic marble and two types of Grytdal soapstone.

Also, for the purpose of determining in reasonable time the degradation phenomena parameters that drive the erosion simulation, Low-cost, small scale, automated erosion chambers for studying accelerated weathering effects on stones were successfully designed, constructed and used. The weathered stone samples were exhaustively characterized by employing a wide range of analytical techniques and approaches that have provided valuable information on the weathering processes and mechanisms.

Although the design of the "Erosion Simulator" software is in its final stage, there are still some unsolved issues that have to be addressed. These mostly come from the fact that the interpretation of the results from the accelerated weathering experiments on the marble and soapstone at macroscopic and microscopic levels is still in progress, and although we can infer that the investigation conducted has given an insight into the changes occurring during erosion/weathering of these stones, the difficulties for incorporating these qualitative results in a quantitative simulation model still remain.

Some of the challenges that we faced and have to be addressed in future work are the following:

- ICP registration is not sufficient. By minimising the overall registration error, it "misses" the possible erosion "common" to all points. For this reason, it is only possible to measure relative rather than absolute erosion values since there are no external fixed reference points.
- The erosion model, which has been yet implemented in the Erosion Simulator, is only applicable to calcium carbonate stones exposed to acid rain polluted by SO_2 and NO_2.
- The Nidaros slabs exhibited an unexpected swelling behaviour in both acid solution chambers; this has not yet been interpreted or modelled.
- The per-mineral recession rates of the stones exposed in the chemical erosion chambers seem quite chaotic and difficult to be related to the experimental parameters of the erosion chambers.
- The environmental parameters and real exposure times used by the model have not yet been related to the physico-chemical parameters of the and exposure times of the accelerated erosion chambers.

6 Acknowledgments

This research is part of the PRESIOUS project and has received funding from the European Unions Seventh Framework Programme STREP Project under grant agreement no 600533.

Stone Samples			
Stone		Material	Experiment
EL1	Elefsis Large 01	*Pentelic Marble*	$Freeze - Thaw$
EL2	Elefsis Large 02	*Pentelic Marble*	*Salt*
EL3	Elefsis Large 03	*Pentelic Marble*	H_2SO_4+HNO_3(aq) *Acid*
ES1	Elefsis Small 01	*Pentelic Marble*	H_2SO_4(aq) *Acid*
NBL1	Nidaros Bad Large 01	*Grytdal Soapstone*	$Freeze - Thaw$
NBL2	Nidaros Bad Large 02	*Grytdal Soapstone*	*Salt*
NBL3	Nidaros Bad Large 03	*Grytdal Soapstone*	H_2SO_4+HNO_3(aq) *Acid*
NBS1	Nidaros Bad Small 01	*Grytdal Soapstone*	*Salt*
NGL1	Nidaros Good Large 01	*Grytdal Soapstone*	$Freeze - Thaw$
NGL2	Nidaros Good Large 02	*Grytdal Soapstone*	*Salt*
NGL3	Nidaros Good Large 03	*Grytdal Soapstone*	H_2SO_4+HNO_3(aq) *Acid*
NGS1	Nidaros Good Small 01	*Grytdal Soapstone*	H_2SO_4(aq) *Acid*

Table 1. Stone samples labeling, material and associate experiment.

Mass Loss Δm (gr)					
Stone		m_1 gr	m_2 gr	Δm gr	$\Delta m/m$ %
EL1	$Freeze - Thaw$	29.1283	29.0847	-0.0436	-0.15
EL2	*Salt*	25.0409	24.8459	-0.1950	-0.78
EL3	*Acid* H_2SO_4+HNO_3(aq)	27.7475	27.5328	-0.2147	-0.77
ES1	*Acid* H_2SO_4(aq)	27.8519	27.5989	-0.2530	-0.91
NBL1	$Freeze - Thaw$	169.2780	168.8975	-0.3805	-0.22
NBL2	*Salt*	195.8884	188.9025	-6.9859	-3.57
NBL3	*Acid* H_2SO_4+HNO_3(aq)	140.1745	139.3690	-0.8055	-0.57
NBS1	*Acid* H_2SO_4(aq)	29.9790	29.6084	-0.3706	-1.24
NGL1	$Freeze - Thaw$	101.7920	101.7464	-0.0456	-0.04
NGL2	*Salt*	161.2788	160.5487	-0.7301	-0.45
NGL3	*Acid* H_2SO_4+HNO_3(aq)	143.4905	143.2244	-0.2661	-0.19
NGS1	*Acid* H_2SO_4(aq)	20.7092	20.6273	-0.0819	-0.40

Table 2. Measurements of the mass loss for the different stone slabs. m_1 initial mass (Round 01), m_2 mass after 1st erosion cycle (Round 02).

Mean Erosion δ (mm)						
Stone		V_1 cm^3	V_2 cm^3	ΔV cm^3	S cm^2	δ mm
EL1	$Freeze - Thaw$	10.8250	10.7281	-0.0969	31.3598	-0.0309
EL2	*Salt*	9.3050	9.1773	-0.1277	28.3975	-0.0450
EL3	*Acid* H_2SO_4+HNO_3(aq)	10.2961	10.1391	-0.1570	29.7689	-0.0527
ES1	*Acid* H_2SO_4(aq)	10.3216	10.1510	-0.1706	29.9718	-0.0569
NBL1	$Freeze - Thaw$	$^{(*)}$61.9314	61.7922	-0.1392	120.5537	-0.0115
NBL2	*Salt*	70.3382	68.6979	-1.6403	126.5692	-0.1296
NBL3	*Acid* H_2SO_4+HNO_3(aq)	49.6610	50.6684	1.0074	97.4351	0.1034
NBS1	*Acid* H_2SO_4(aq)	10.8753	11.1004	0.2251	32.9741	0.0683
NGL1	$Freeze - Thaw$	$^{(*)}$35.4548	35.4389	-0.0159	72.1983	-0.0022
NGL2	*Salt*	$^{(*)}$55.5347	55.2833	-0.2514	102.9147	-0.0244
NGL3	*Acid* H_2SO_4+HNO_3(aq)	49.2560	49.3007	0.0447	103.6453	0.0043
NGS1	*Acid* H_2SO_4(aq)	7.1383	7.1294	-0.0089	24.6578	-0.0036

Table 3. Computation of the mean erosion for the different stone slabs: (a) Cubic volume approximation; and (b) Surface area approximation. $^{(*)}$ Volume V_1 computed from mass m_1 using density ρ_2 considered constant.

References

AICON 3D systems (2015), 'http://aicon3d.com/start.html'.

Arduino LLC (2015), 'http://www.arduino.cc/'.

Besl, P. J. & McKay, N. D. (1992), 'A method for registration of 3-D shapes', *IEEE Trans. Pattern Anal. Mach. Intell.* **14**(2), 239–256.

Doehne, E. & Price, C. A. (2010), Stone conservation: An overview of current research, Technical report, Getty Conservation Institute, Los Angeles, US.

Gauri, K. L. & Bandyopadhyay, J. K. (1999), *Carbonate Stone, Chemical Behaviour, Durability and Conservation*, John Wiley & Sons, Inc.

Massey, S. (1999), 'The effects of ozone and {NOx} on the deterioration of calcareous stone', *Science of The Total Environment* **227**(2–3), 109–121.

Moropoulou, A., Bisbikou, K., Torfs, K., van Grieken, R., Zezza, F. & Macri, F. (1998), 'Origin and growth of weathering crusts on ancient marbles in industrial atmosphere', *Atmospheric Environment* **32**(6), 967–982.

Price, D. G. (1995), 'Weathering and weathering processes', *Quarterly Journal of Engineering Geology and Hydrogeology* **28**(3), 243–252.

Robertson CGG (2015), 'http://www.robertson-cgg.com/'.

Schellewald, C., Theoharis, T., Gebremariam, K. F. & Kvittingen, L. (2013), State of the art report on deterioration simulation, Technical Report PRESIOUS-D3.1, NTNU, Trondheim, Norway.

Scherer, G. (2006), Internal stress and cracking in stone and masonry, *in* M. KONSTA-GDOUTOS, ed., 'Measuring, Monitoring and Modeling Concrete Properties', Springer Netherlands, pp. 633–641.

Storemyr, P. (1997), The stones of Nidaros: an applied weathering study of Europe's northernmost medieval cathedral, PhD thesis, Norwegian University of Science and Technology (NTNU).

Storemyr, P. (2004), 'Weathering of soapstone in a historical perspective', *Materials Characterization* **53**, 191–207.

Storemyr, P., Wendler, E. & Zehnder, K. (2001), Weathering and conservation of soapstone and greenschist used at Nidaros Cathedral (Norway), *in* A. Lunde, Ø. & Gunnarsjaa, ed., 'Report Raphael II Nidaros Cathedral Restoration Trondheim Norway 2000.', EC Raphael Programme – European Heritage Laboratory.

Varotsos, C., Tzanis, C. & Cracknell, A. (2009), 'The enhanced deterioration of the cultural heritage monuments due to air pollution', *Environ Sci Pollut Res* **16**, 590–592.

Yerrapragada, S., Chirra, S., Jaynes, J., Li, S., Bandyopadhyay, J. & Gauri, K. (1996), 'Weathering rates of marble in laboratory and outdoor conditions', *Journal of Environmental Engineering* **122**(9), 856–863.

Yerrapragada, S. S., Jaynes, J. H., Chirra, S. R. & Gauri, K. L. (1994), 'Rate of weathering of marble due to dry deposition of ambient sulfur and nitrogen dioxides', *Analytical Chemistry* **66**(5), 655–659.